Accepted Manuscript

Electrochemical detection of *Salmonella* using an *invA* genosensor on polypyrrole-reduced graphene oxide modified glassy carbon electrode and AuNPs-horseradish peroxidase-streptavidin as nanotag

Yongkang Ye, Wuwen Yan, Yaqian Liu, Shudong He, Xiaodong Cao, Xuan Xu, Haisong Zheng, Sundaram Gunasekaran

PII: S0003-2670(19)30556-2

DOI: https://doi.org/10.1016/j.aca.2019.05.012

Reference: ACA 236775

To appear in: *Analytica Chimica Acta*

Received Date: 15 April 2019

Revised Date: 3 May 2019

Accepted Date: 5 May 2019

Please cite this article as: Y. Ye, W. Yan, Y. Liu, S. He, X. Cao, X. Xu, H. Zheng, S. Gunasekaran, Electrochemical detection of *Salmonella* using an *invA* genosensor on polypyrrole-reduced graphene oxide modified glassy carbon electrode and AuNPs-horseradish peroxidase-streptavidin as nanotag, *Analytica Chimica Acta*, https://doi.org/10.1016/j.aca.2019.05.012.

Electrochemical detection of *Salmonella* using an *invA* genosensor on polypyrrole-reduced graphene oxide modified glassy carbon electrode and AuNPs-horseradish peroxidase-streptavidin as nanotag

Yongkang Ye [a], Wuwen Yan [a], Yaqian Liu [a], Shudong He [a], Xiaodong Cao [a, *], Xuan Xu [b], Haisong Zheng [c], Sundaram Gunasekaran [d, **]

[a] *School of Food Science and Engineering, Hefei University of Technology, Hefei 230009, China.*

[b] *College of Chemistry and Molecular Engineering, Nanjing Tech University, Nanjing 211816, China*

[c] *Technology Center of Anhui Entry-Exit Inspection and Quarantine Bureau, Hefei 230032, China*

[d] *Department of Biological Systems Engineering, University of Wisconsin-Madison, Madison, WI 53706, USA*

[*] Corresponding author.

[**] Corresponding author.

E-mail addresses: xiaodongcao@hfut.edu.cn (X. Cao), guna@wisc.edu (S. Gunasekaran)

Abstract: A rapid and sensitive electrochemical biosensor was constructed to detect *Salmonella* using *invA* gene biosensor. The biosensing was based on polyrrole-reduced graphene oxide (PPy-rGO) nanocomposite modified glassy carbon electrode (GCE) and signal amplification with horseradish peroxidase-streptavidin biofunctionalized gold nanoparticles (AuNPs-HRP-SA). PPy-rGO was prepared at 60 □ by chemical reduction of PPy-functionalized graphene oxide (PPy-GO) that was synthesized by *in situ* polymerization at room temperature. The detection signal was amplified via enzymatic reduction of H_2O_2 in the presence of hydroquinone (HQ) using AuNPs-HRP-SA as nanotag. Under optimal conditions, the differential pulse voltametric (DPV) signal from the biosensor was linearly related to the logarithm of target *invA* gene concentrations from 1.0×10^{-16} to 1.0×10^{-10} M, and the limit of detection (LOD) was 4.7×10^{-17} M. The biosensor can also detect *Salmonella* in the range of 9.6 to 9.6×10^{4} CFU mL^{-1}, with LOD of 8.07 CFU mL^{-1}. The biosensor showed good regeneration ability, acceptable selectivity, repeatability and stability, which bode well as an alternative method for *Salmonella* screening.

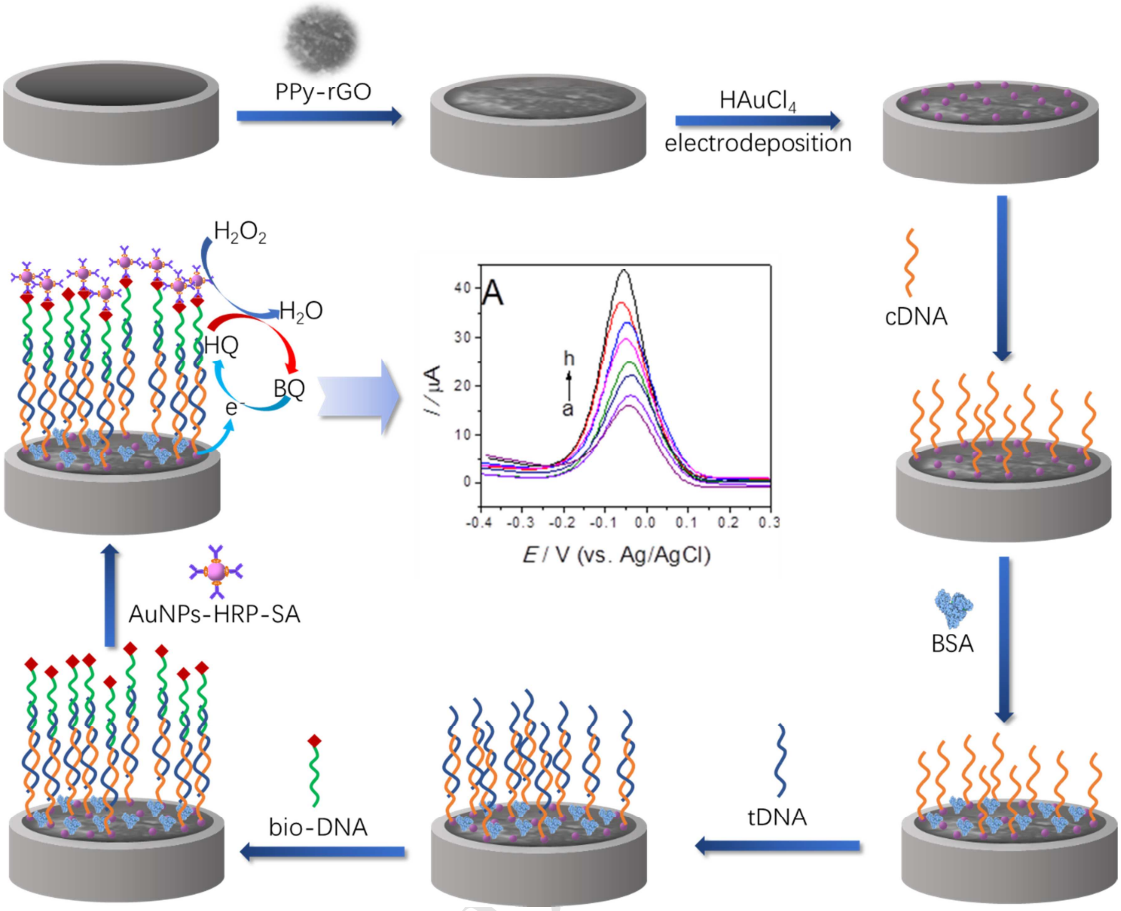
PPy-rGO
HAuCl4
electrodeposition
cDNA
BSA
tDNA
bio-DNA
AuNPs-HRP-SA
H2O2
H2O
HQ
BQ
e
A
h
a
I / μA
E / V (vs. Ag/AgCl)

Electrochemical detection of *Salmonella* using an *invA* genosensor on polypyrrole-reduced graphene oxide modified glassy carbon electrode and AuNPs-horseradish peroxidase-streptavidin as nanotag

Yongkang Ye [a], Wuwen Yan [a], Yaqian Liu [a], Shudong He [a], Xiaodong Cao [a, *], Xuan Xu [b], Haisong Zheng [c], Sundaram Gunasekaran [d, **]

[a] *School of Food Science and Engineering, Hefei University of Technology, Hefei 230009, China.*

[b] *College of Chemistry and Molecular Engineering, Nanjing Tech University, Nanjing 211816, China*

[c] *Technology Center of Anhui Entry-Exit Inspection and Quarantine Bureau, Hefei 230032, China*

[d] *Department of Biological Systems Engineering, University of Wisconsin-Madison, Madison, WI 53706, USA*

[*] Corresponding author.

[**] Corresponding author.

E-mail addresses: xiaodongcao@hfut.edu.cn (X. Cao), guna@wisc.edu (S. Gunasekaran)

Abstract: A rapid and sensitive electrochemical biosensor was constructed to detect *Salmonella* using *invA* gene biosensor. The biosensing was based on polyrrole-reduced graphene oxide (PPy-rGO) nanocomposite modified glassy carbon electrode (GCE) and signal amplification with horseradish peroxidase-streptavidin biofunctionalized gold nanoparticles (AuNPs-HRP-SA). PPy-rGO was prepared at 60 □ by chemical reduction of PPy-functionalized graphene oxide (PPy-GO) that was synthesized by *in situ* polymerization at room temperature. The detection signal was

amplified via enzymatic reduction of H_2O_2 in the presence of hydroquinone (HQ) using AuNPs-HRP-SA as nanotag. Under optimal conditions, the differential pulse voltametric (DPV) signal from the biosensor was linearly related to the logarithm of target *invA* gene concentrations from 1.0×10^{-16} to 1.0×10^{-10} M, and the limit of detection (LOD) was 4.7×10^{-17} M. The biosensor can also detect *Salmonella* in the range of 9.6 to 9.6×10^{4} CFU mL^{-1}, with LOD of 8.07 CFU mL^{-1}. The biosensor showed good regeneration ability, acceptable selectivity, repeatability and stability, which bode well as an alternative method for *Salmonella* screening.

Keywords: *Salmonella*; *invA* gene; polypyrrole-reduced graphene oxide nanocomposite; electrochemical biosensor; horseradish peroxidase-streptavidin biofunctionalized gold nanoparticles.

1. Introduction

Salmonella, a gram-negative enteric bacilli and zoonotic foodborne pathogen, is a major pathogen implicated in foodborne disease outbreaks [1,2]. Within 12-72 h after consuming *Salmonella*-contaminated foods, humans, especially children and the elderly, may experience severe symptoms and health risks [3]. Therefore, there is an urgent need for rapid and sensitive detection of *Salmonella* in monitoring food safety and clinical diagnosis.

Currently, there are two major methods for detection of *Salmonella*. One is the traditional culture method [4], which is a labor-intensive and time-consuming method that requires up to 5–7 days to get results. The other is instrumental analysis method, which includes polymerase chain reaction (PCR) [5,6], spectroscopic biosensing [7,8] and electrochemical biosensing [9-11]. With the rapid development of nanotechnology, the detection time for *Salmonella* can be greatly decreased, while the sensitivity for *Salmonella* can be dramatically improved [9,12,13]. In the past decades, numerous electrochemical biosensing methods have been developed because of their several advantages [14], including improved sensitivity due to the use of various nanomaterials [9-11,13]. For instance, an aptasensor was developed for sensitive detection of *Salmonella typhimurium* (16 CFU mL^{-1}) by target-induced aptamer displacement on gold nanoparticles (AuNPs) deposited gold electrode with rolling circle amplification (RCA) [13].

The use of conducting polymers is popular in biosensor fabrication due to their excellent electrical properties [15,16]. Different conducting polymers of various morphologies and structures have been synthesized [17-19]. Polypyrrole (PPy), a promising conducting polymers, synthesized from pyrrole monomer, finds wide application in the fields of supercapacitors [20-22], water treatment [23,24], catalysis [24,25], energy storage [19], sensing device [26] and sensing platform [27-29]. PPy and its nanocomposite with other nanostructures can be synthesized by chemical polymerization [29] or electropolymerization [22,30]. The chemical polymerization is usually done at a low temperature (0-5□) in an acid solution using oxidants such as $FeCl_3$ [25,31], 1,4-benzoquinone [32] and ammonium persulfate (APS) [23,33]. Some researchers prepared PPy and its nanocomposite by chemical polymerization without adjusting the pH value of the reaction solution [34,35], without addition of oxidant [19], or under a condition with relatively higher temperature [19,27,32]. For example, PPy-functionalized reduced graphene oxide (PPy-rGO) nanomaterial was prepared by drop casting *in situ* oxidative polymerization on the surface of rGO sheets using APS as oxidant at room temperature [27]. The prepared PPy-rGO film on a glass substrate was used to gas (ammonia) sensing with high sensitivity of 3 ppm.

Due to the good biocompatibility, facile preparation and ease of modification, AuNPs are widely used in biosensors [10,36]. Herein, enlightened by the reported method [27,34,35] we prepared PPy decorated graphene oxide (PPy-GO) nanocomposite by *in situ* oxidative polymerization of pyrrole monomer on the surface of GO sheets at room temperature. Further chemical reduction at 60 □ was employed

to obtain PPy-rGO nanocomposite [37]. The prepared PPy-rGO was then used to fabricate the sensing interface for *Salmonella*. The *invA* gene sequences, a highly conserved gene in *Salmonella*, was selected as the target to determine *Salmonella* content in CFU mL^{-1}. We achieved a rapid and sensitive biosensing method the detection for *Salmonella* by combining the good electrical property of PPy-rGO with the signal amplification of AuNPs-horseradish peroxidase-streptavidin (AuNPs-HRP-SA) nanotag.

2. Experimental

2.1 Materials and reagents

The graphite oxide was purchased from Nanjing JCNANO Technology Co., LTD. (Nanjing, China). Pyrrole (Py) purchased from Aladdin Industrial Co., Ltd. (Shanghai, China) was distilled and kept at 4 □ in dark. Chloroauric acid ($HAuCl_4 \cdot 4H_2O$) was ordered from National Medicine Group Shanghai Chemical Reagent Co., Ltd. (Shanghai, China). Horseradish peroxidase-conjugated streptavidin (HRP-SA) was purchased from Shanghai SXBIO Biotech Co., Ltd. (Shanghai, China). Bovine albumin (BSA) and Trans 2 K Plus Marker were purchased from TransGen Biotech Co., Ltd. (Beijing, China). Taq DNA polymerase, dNTP mixture, 10 × PCR buffer and Luria-Bertani broth were ordered from Shanghai Sangon Biotechnology Co., Ltd. (Shanghai, China). All reagents are stored under appropriate conditions according to the instructions. The buffers or solutions used in this study were prepared using ultrapure water and shown in the **Table S1**. Ultrapure water was used throughout the experiments.

All DNA sequences were synthesized and purified by Shanghai Sangon Biotechnology Co., Ltd. (Shanghai, China), and their sequences are shown in the **Table S2**.

Salmonella typhimurium strains were obtained from the Anhui Entry-exit Inspection and Quarantine Bureau.

2.2 Instruments

The morphology of the materials was analyzed with scanning electron microscope (SEM, SU8020, Hitachi, Japan) at an accelerating voltage of 3.0 kV. X-ray photoelectron spectroscopy (XPS) analysis was conducted on ESCALAB250 X-ray photoelectron spectrometer (Thermo Fisher Scientific, USA) using an Al Kα (1486.6 eV) radiation at a power of 225 W. UV-vis absorption spectra were obtained on a UV-4802 spectrophotometer (Unico Shanghai Instrument Co., Ltd., Shanghai, China). The PCR amplification was carried out on TC-96/T/H (Hangzhou Bioer Technology Co., Ltd., Hangzhou, China).

Electrochemical experiments were performed on a CHI660D electrochemical work station (Shanghai Chenhua Instrument Co., Ltd., China) with a standard three-electrode configuration. A platinum wire was employed as the auxiliary electrode, an Ag/AgCl electrode was served as the reference electrode, and a modified glassy carbon electrode (GCE, 3 mm in diameter) was used as the working electrode.

2.3 Preparation of PPy-rGO

Graphene oxide (GO) was firstly prepared as the source material of rGO according to our previous work [38]. The PPy-rGO was prepared in two steps. Step 1 is *in situ* polymerization without using acid. Typically, 10.0 mL of GO (1.0 mg mL^{-1}) was sonicated for 10 min, followed by adding 150 μL of pyrrole monomer (dissolved in 10 mL ethanol). The mixture was sonicated for another 30 min. Then 10.0 mL of $FeCl_3$ (0.5 mol L^{-1}) was dropwise added into the above mixture under stirring. The suspension was stirred for 24 h at room temperature to obtain PPy-GO by oxidative polymerization. The PPy-GO was washed with ethanol for several times to remove excess pyrrole monomer, and then dried at 60 □ for 12 h. Step 2 is synthesis of PPy-rGO by chemical reduction. Briefly, 10.0 mL of PPy-GO (1.0 mg mL^{-1}) was put into a three-neck flask, followed by adding 100 μL of ammonia (28%, w/w) and 40 μL of hydrazine hydrate (25%, w/w) under stirring. The mixture was then left reacting and refluxing for 16 h at 60 □. The obtained black precipitate (PPy-rGO) was separated by centrifugation and then washed with ethanol and water several times. The purified PPy-rGO was finally dried under vacuum and stored for later use.

2.4 Preparation of AuNPs-HRP-SA conjugates

AuNPs of an average size of 10 nm (see Electronic Supplementary material **Fig. S1**) was synthesized according to our previous work [10]. The AuNPs-HRP-SA was prepared by absorbing HRP-SA on the surface of AuNPs. Typically, 1.0 mL of AuNPs was centrifuged at 10,000 rpm for 30 min. After discarding the supernatant, the obtained precipitate was dispersed with 0.1 M PBS (pH 7.4) to a volume of 300 μL.

Afterwards, 20 μL of 100 μg mL^{-1} HRP-SA was added into the concentrated AuNPs solution. The mixture was kept shaking for 24 h at 4 °C. The unattached HRP-SA was isolated from AuNPs-HRP-SA by centrifugation (10,000 rpm, 30 min) and washed with PBS (0.1 M pH 7.4) for three times. The obtained AuNPs-HRP-SA was dispersed with PBS (0.1 M pH 7.4) to a volume of 300 μL and stored in frig at 4 °C for later use. The size of AuNPs-HRP-SA was barely changed during the process (see Electronic Supplementary material **Fig. S2**).

2.5 Construction of invA gene sensor

Prior to use, bare GCE was sequentially polished to obtain a mirror-like surface with 1.0, 0.3 and 0.05 μm alumina powder, followed with ultrasonic cleaning with ethanol and water in turn, and then dried thoroughly under a nitrogen steam. Then, 5 μL of PPy-rGO suspension (1.0 mg mL^{-1}) was dropped onto the pretreated GCE and kept in a desiccator drying for 2 h to obtain PPy-rGO modified GCE (named as PPy-rGO/GCE). Subsequently, the AuNPs was electrodeposited on PPy-rGO/GCE in a solution of 0.1 M KNO_3 containing 3.0 mM $HAuCl_4$ via amperometry at a potential of −0.2 V for 70 s. The obtained electrode was then washed with water and dried with nitrogen to obtain depAuNPs modified GCE (depAuNPs/PPy-rGO/GCE). Next, 5 μL of 10 μM cDNA was dropped on the depAuNPs/PPy-rGO/GCE and the modified electrodes were incubated at 4 □ for 12 h. After thoroughly rinsing with 0.1% SDS solution and Tris-HCl (10 mM, pH 7.4) solution, the nonspecific binding sites on cDNA/depAuNPs/PPy-rGO/GCE were blocked with BSA (1 mM) for 30 min [39].

2.6 Hybridization and electrochemical measurement

Hybridization was accomplished by immersing cDNA/depAuNPs/PPy-rGO/GCE in mixed solution consisted of various concentrations of tDNA (100 μL) and bio-DNA (10 μL, 10 μM), and incubating at 37 °C for 1 h. On this electrode (bio-DNA/tDNA/cDNA/depAuNPs/PPy-rGO/GCE) 5 μL AuNPs-HRP-SA was dropped, and incubated at room temperature for 30 min. It was rinsed thoroughly with buffer and dried with N_2 stream. The modified electrode was named as AuNPs-HRP-SA/bio-DNA/tDNA/cDNA/ depAuNPs/PPy-rGO/GCE.

Cyclic voltammetry (CV) was conducted to characterize the construction process of the biosensor in 5.0 mM $[Fe(CN)_6]^{3-/4-}$ solution containing 0.1 M KCl. The measurements were performed in a potential ranging from −0.1 to 0.7 V at a scan rate of 50 mV s^{-1}.

The differential pulse voltammetry (DPV) measurements for the detection of tDNA were performed in 0.1 M PBS (pH7.4) containing 2.0 mM HQ and 3.0 mM H_2O_2. The DPV curves were recorded in the potential window of −0.6 to 0.6 V at a scan rate of 4 mV s^{-1}; pulse amplitude was 50 mV and pulse width was 0.05 s.

2.7 Preparation of real samples and PCR product of the invA gene sequence

The activated *Salmonella* strains were first inoculated into Luria-Bertani medium at 37 °C for 24 h. Then the bacterial broth was centrifuged at 10,000 rpm at 4 □ for 5 min. The precipitate was collected and washed with water, and then resuspended in

water. The enumeration of viable *Salmonella* was conducted by plating 100 μL of various concentrations of dilutions onto plate count agar. The plates were then incubated for 24 h at 37 °C, and the culture colonies on these plates were numerated to estimate the number of viable *Salmonella* in CFU mL^{-1}.

For the detection of *invA* sequences in real samples, total DNA sequences in the above cultivated *Salmonella* with various concentrations were extracted and used as PCR template. In brief, the *Salmonella* with various concentrations were boiled at 100 °C for 15 min and then chilled on ice immediately following with centrifugation at 10,000 rpm for 5 min at 4 □. The supernatants containing genome DNA were collected and kept at -20 □ for further experiment.

PCR was applied to amplify the extracted DNA. Five micro liters of 10×PCR buffer, 5.0 μL genomic DNA, 1.0 μL of forward and reverse primers (10 μM), 1.0 μL of Taq DNA polymerase (5 U μL^{-1}), 1.0 μL of dNTP (10 mM each), 3.0 μL of $MgCl_2$ (25 mM), and 33 μL of H_2O composed the PCR mixture. The amplification parameters were set as follows: denaturation at 94 °C for 5 min, followed by 30 cycles of 94 °C for 30 s, annealing at 57 °C for 30 s, extension at 72 °C for 30 s, and final extension at 72 °C for 4 min. The PCR products were detected by running PCR mixtures (10.0 μL) in 1% agarose gel for 20 min and observed under ultraviolet light.

3. Results and discussion

3.1 Characterizations of PPy-rGO

The morphological characteristics of GO, rGO and PPy-rGO were characterized by SEM, and the images are shown in **Fig. 1**. The SEM images of GO (**Fig. 1** A) and rGO (**Fig. 1** B) show flake-like and crumpled morphology. While PPy was polymerized on the surface of rGO sheets, the surface of rGO became rough (**Fig. 1** C). The granular-like PPy particles nearly covered the entire rGO sheet. This demonstrates the formation of PPy-rGO.

The elemental compositions and chemical states of GO, PPy-GO and PPy-rGO were determined by XPS. As seen in **Fig. 2** A, two major peaks associated with O1s (532.43 eV) and with C1s (284.78 eV), are present in the spectrum of GO. An obvious peak at 400.10 eV corresponding to N1s can be found in the full survey of PPy-GO (**Fig. 2** C) and PPy-rGO (**Fig. 2** E). The atomic ratios of nitrogen atom in GO, PPy-GO and PPy-rGO were about 1.86%, 7.32% and 9.89%, respectively. In addition, the ratio of C to O in GO and PPy-rGO were about 1.68 and 4.11, respectively. These variations indicate the removal of oxygen group, the reduction of GO, and the formation of PPy-rGO.

The C1s spectra of GO, PPy-GO and PPy-rGO were processed using XPSPEAK41 software, and the fitted curves are displayed in **Fig. 2** B, D, and F. The four peaks observed in C1s of GO (**Fig. 2** B) can be assigned to π-π stacking of GO sheets (293.56 eV), O-C=O (288.90 eV), C-O (286.99 eV), and C-C/C=C (284.76 eV) [22,40,41]. When pyrrole was polymerized using $FeCl_3$ as oxidant, a new peak at about 285.80 eV is present in C1s spectrum of PPy-GO, which is allocated to C-N

bond (**Fig. 2** D) [31]. Furthermore, the intensity of π-π stacking was greatly increased. The results indicate that pyrrole attached onto the surface of GO via π-π stacking during the sonication procedure and then polymerized on GO sheets when $FeCl_3$ was applied as oxidant. In terms of the C1s spectrum of PPy-rGO (**Fig. 2** F), the peak of C-N bond still can be observed, while the peak resulted from π-π stacking interaction nearly vanished, indicating PPy attached on the surface of rGO sheets through hydrogen bond. The intensities of non-oxygenated ring C (C-C/C=C) in carbon atoms in various functional groups in GO and PPy-rGO were estimated to be 46.8% and 62.6%, respectively, which can also confirm the removal of oxygen and the reduction of GO. The XPS results demonstrate that PPy-rGO was successfully synthesized.

The UV-vis spectrum of GO (**Fig. 3**, curve a) gave an obvious peak at ~232 nm, which attributed to π-π* transitions of aromatic rings in GO sheets. There was a shoulder peak located at 300 nm, corresponding to n-π* transitions of C=O bonds [38,41]. The absorbance at 232 nm shifted to 280 nm (**Fig. 3**, curve c), indicating the reduction of GO and the formation of rGO [38,42]. A broad and intense absorbance in the region 200-270 nm and an absorbance peak at ~281 nm were observed in the spectrum of PPy-GO (**Fig. 3**, curve b), which are attributed to π-π* transition of benzenoid ring in PPy chain and GO sheets [43]. There was also a weak absorbance at 331 nm, which is associated with polaron transitions in PPy [27,44]. When PPy-GO was treated with reducing agent, two distinct peaks at 203 nm and 271 nm were observed (**Fig. 3**, curve d). The absorption band at 203 nm (E_2 band) attributed to π-π* transition of C=C bond. Whereas, the absorption band at 271 nm may due to the

244 characteristic absorption of rGO [35] or the conjugation of the molecular in PPy [45].
245 The blueshifts of these bands may be due to the strong interaction between PPy and
246 rGO sheets via hydrogen bonds.

247 *3.2 Sensing principle for invA gene of Salmonella*

248 The prepared PPy-rGO nanocomposite was used to construct the sensing
249 interface for detection of *invA* gene of *Salmonella*, and the sensing principle was
250 illustrated in **Scheme 1**. As can be seen from the scheme, the biosensor was
251 constructed step by step. CV was applied to stepwise characterize each fabrication
252 procedure in 5.0 mM $[Fe(CN)_6]^{3-/4-}$ containing 0.1 M KCl (**Fig. 4**A). A pair of
253 well-defined redox peaks belonging to Fe^{3+}/Fe^{2+} can be observed with different GCEs
254 with varied peak currents. The absolute value of the peak currents increased gradually
255 with the modification of PPy-rGO (**Fig. 4**A, curve b), and subsequently with
256 depAuNPs (**Fig. 4**A, curve c), when compared with those obtained at bare GCE (**Fig.**
257 **4**A, curve a). These demonstrate PPy-rGO and depAuNPs facilitated the electron
258 transfer of Fe^{3+}/Fe^{2+}. Thereafter, the absolute value of the peak current decreased
259 along with the advancing fabrication process of the biosensor (**Fig. 4**A, curve d and e).
260 When the biosensor was applied to detect tDNA by hybridizing with the mixture of
261 tDNA and bio-DNA (**Fig. 4**A, curve f), and the signal tag of AuNPs-HRP-SA (**Fig. 4**A,
262 curve g), the values of the peak currents further decreased. The CV result indicates the
263 successful construction of the *invA* gene sensor.

The sensitive detection for *invA* in *Salmoella* was achieved by the amplified signal of the reduction of H_2O_2 in presence of HQ, which was confirmed by using DPV measurements (**Fig. 4**B). The constructed biosensor showed a DPV response when there was no tDNA in the hybridization mixture (**Fig. 4**B, curve a). It was due to the electrocatalytic ability of the applied PPy-rGO to the reduction of H_2O_2. It can be taken as the blank signal. When the biosensor was used in detecting tDNA (100 pM) without conducting the specific reaction between bio-DNA and AuNPs-HRP-SA, the obtained signal on the detecting interface was similar to the blank signal (**Fig. 4**B, curve b). The biosensor showed the strongest response when a specific interaction occurred between bio-sDNA and AuNPs-HRP-SA nanotag (**Fig. 4**B, curve c). The response on the biosensor decreased without using AuNPs as carriers for immobilization of HRP-SA (**Fig. 4**B, curve d). In addition, the response on cDNA/depAuNPs/rGO/GCE further decreased when using HRP-SA as signal tag only (**Fig. 4**B, curve e). Furthermore, the DPV current of curve c was 2.2 times that of curve e, indicating the amplified signal in the present detecting strategy. This may be due to the facilitation of electron transfer of PPy-rGO and the use of AuNPs as carrier for immobilizing a large amount of HRP-SA.

3.3 Analytical performance of the biosensor

In order to achieve the best analytical performance of the *invA* gene sensor, the experimental parameters including the pH value of the detecting buffer, the hybridization time between cDNA and the mixture of tDNA and bio-DNA, the time of

the specific reaction between bio-DNA and AuNPs-HRP-SA, and the concentration of the added HQ and H_2O_2, were optimized using DPV measurements (**Fig. S3**). As can be conclude from the figure, the biosensor reached its best analytical performance under the conditions as follows: 0.1 M PBS with a pH value of 7.4, hybridization time of 60 min, specific reaction time of 30 min, 2.0 mM of the added HQ, and 3.0 mM of the added H_2O_2.

Under the optimal reaction conditions, the DPV responses obtained with different tDNA concentrations are shown in **Fig. 5**A. The peak current (I) increased linearly with the increasing logarithmic concentration of tDNA (log C) in the range of 1.0×10^{-16} to 1.0×10^{-10} M (**Fig. 5**B). The corresponding regression equation was written as I (μA) = 3.81 log$C$ (M) + 78.28 (R = 0.996), and the LOD was 4.7×10^{-17} M (S/N = 3). The analytical performance of the biosensor was better than that of our previously reported method [10]. The achieved sensitivity may be attributed to the signal amplifications from PPy-rGO and AuNPs-HRP-SA.

The regeneration ability of the biosensor was tested by unwinding the hybridized double-stranded DNA through incubating the used electrode in 90 □ water for 5 min, and then rapidly subjecting into a salt ice water. After washing with PBS buffer and water for several times, the revived biosensor was used to detect tDNA by repeating the hybridization and specific reaction that involved in the detecting procedure. We found that the DPV signal towards 100 pM of tDNA maintained 91.6% of its initial

response after three cycles of the regeneration (**Fig. 5**C and D). This indicates the good regeneration ability of the biosensor.

3.4 Specificity and repeatability of the biosensor

The selectivity of the biosensor was investigated by detecting single base mismatched (Mis-1, 1 nM), three bases mismatched (Mis-3, 1 nM), and non-complementary (Non-C, 1 nM) DNA sequences, and the recorded responses of these sequences were compared with that of tDNA (100 pM) (**Figs. 6** A and B). The DPV of tDNA was the most intensive among these sequences. The biosensor showed negligible responses to Mis-3 and Non-C sequence, and non-negligible response to Mis-1, when the concentrations of these sequences were 10 times than that of tDNA. This demonstrates an acceptable selectivity of the proposed biosensor.

To investigate the repeatability of the biosensor, three GCEs were used to fabricate and detect tDNA with a concentration of 1 pM. The measurements were repeated for 3 times. The relative standard deviation (RSD) of each fabricated biosensor was less than 5%, and the RSD of the three biosensors was about 7.98%. After a storage at 4 °C for 7 days, the responses on these biosensors maintained 84.6% of the original signals. These demonstrate acceptable reproducibility and stability of the proposed biosensor.

3.5 Detection of Salmonella in real samples

The feasibility of the constructed biosensor for detection of *Salmonella* in actual samples was evaluated by detecting the PCR product using the extracted total DNA as template from various concentration of *Salmonella*. **Fig. 6**C shows the agarose gel electrophoresis detection of PCR products. As can be seen from **Fig. 6**C, a DNA fragment of 284 bases (*invA* gene segment) in length can be detected effectively only when the concentration of *Salmonella* was no less than 9.6×10^4 CFU mL^{-1} (**Fig. 6**C, lane 4). At the same time, our constructed biosensor was also applied to determine the denatured PCR products for *Salmonella* (0 to 9.6×10^4 CFU mL^{-1}). The DPV responses obtained on the biosensor toward different PCR samples for *Salmonella* are shown in **Fig. 6**D. It is obvious that the biosensor showed DPV responses to the PCR products of various concentrations of *Salmonella* ranging from 9.6 to 9.6×10^4 CFU mL^{-1}. The good linear relationship between the DPV responses and the logarithm of *Salmonella* concentration (**Fig. 6**D, inset) can be written in an equation as I (μA) = 7.999 log C (CFU mL^{-1}) + 8.107 (R = 0.995), and the LOD was 8.07 CFU mL^{-1}. The analytical performance (linear range, detection limit and time for detection) of our biosensor and other reported biosensors were compared and listed in **Table 1**. The analytical performance of our biosensor was better than those biosensors using spectroscopic methods, and it was comparable to those electrochemical biosensors.

4. Conclusions

In summary, we constructed a biosensor for rapid and sensitive electrochemical detection of *Salmonella* by integrating the good conductivity of PPy-rGO and signal

amplification of AuNPs-HRP-SA. The biosensor showed good sensitivity to tDNA with LOD as low as 4.7×10^{-17} M. Moreover, the gene sensor can be used to detect *Salmonella* within 2 h with LOD of 8.07 CFU mL^{-1}. The biosensor possessed good regeneration ability, acceptable selectivity, repeatability and stability, which allow it to be used as an alternative tool for *Salmonella* screening in monitoring food safety and clinical diagnosis.

Acknowledgment

The project is supported by the National Natural Science Foundation of China (Grant No. 31772099, 31401573 and 21505071), the Natural Science Foundation of Anhui Province (No. 1908085MC98), the Anhui Key Research and Development Program (No. 201904a06020030), and the China Postdoctoral Science Foundation (Grant No. 2016M592050, 2017T100446).

References

[1] R. Luo, Y. Li, X. Lin, F. Dong, W. Zhang, L. Yan, W. Cheng, H. Ju, S. Ding, A colorimetric assay method for invA gene of *Salmonella* using DNAzyme probe self-assembled gold nanoparticles as single tag, Sensor. Actuat. B Chem. 198 (2014) 87–93.

[2] J. Li, X. Sun, R. Li, J. Wang, J. Wang, L. Hu, Development of a quantitative fluorescence single primer isothermal amplification-based method for the detection of *Salmonella*, Int. J. Food Microbiol. 219 (2016) 22–27.

[3] A. Grant, F. Hashem, S. Parveen, *Salmonella* and *Campylobacter*: Antimicrobial resistance and bacteriophage control in poultry, Food Microbiol. 53 (2016) 104–109.

[4] M. Trkov, G. Avguštin, An improved 16S rRNA based PCR method for the specific detection of *Salmonella enterica*, Int. J. Food Microbiol. 80 (2003) 67–75.

[5] K. Gokduman, M. Dilek Avsaroglu, A. Cakiris, D. Ustek, G. Candan Gurakan, Recombinant plasmid-based quantitative Real-Time PCR analysis of *Salmonella enterica* serotypes and its application to milk samples, J. Microbiol. Methods. 122 (2016) 50–58.

[6] A.C. Vinayaka, T.A. Ngo, K. Kant, P. Engelsmann, V.P. Dave, M.A. Shahbazi, A. Wolff, D.D. Bang, Rapid detection of *Salmonella enterica* in food samples by a novel approach with combination of sample concentration and direct PCR, Biosens. Bioelectron. 129 (2019) 224–230.

[7] M. Eady, G. Setia, B. Park, Detection of *Salmonella* from chicken rinsate with visible/near-infrared hyperspectral microscope imaging compared against RT-PCR, Talanta 195 (2019) 313–319.

[8] S. Alamer, S. Eissa, R. Chinnappan, P. Herron, M. Zourob, Rapid colorimetric lactoferrin-based sandwich immunoassay on cotton swabs for the detection of foodborne pathogenic bacteria, Talanta 185 (2018) 275–280.

[9] D. Zhu, Y. Yan, P. Lei, B. Shen, W. Cheng, H. Ju, S. Ding, A novel electrochemical sensing strategy for rapid and ultrasensitive detection of *Salmonella* by rolling circle amplification and DNA-AuNPs probe, Anal. Chim. Acta 846 (2014) 44–50.

[10] Y. Ye, Y. Liu, S. He, X. Xu, X. Cao, Y. Ye, H. Zheng, Ultrasensitive electrochemical DNA sensor for virulence *invA* gene of Salmonella using silver nanoclusters as signal probe, Sensor. Actuat. B Chem. 272 (2018) 53–59.

[11] V.Y. Doan, T. Trung, P.D. Tam, L.T.H. Yen, N.L. Hoang, V.-H. Pham, V. Van Thu, N.T.

Nguyet, H. Lan, A label-free and highly sensitive DNA biosensor based on the core-shell structured CeO_2-NR@Ppy nanocomposite for *Salmonella* detection, Mater. Sci. Eng. C 96 (2019) 790–797.

[12] J. Hu, Y.Z. Jiang, M. Tang, L.L. Wu, H.Y. Xie, Z.L. Zhang, D.W. Pang, Colorimetric-fluorescent-magnetic nanosphere-based multimodal assay platform for *Salmonella* detection, Anal. Chem. 91 (2019) 1178–1184.

[13] G. Yi, W. Nian, L. Li, J. Yang, R. Yuan, H. Zhang, C. Ge, L. Yi, Target-induced aptamer displacement on gold nanoparticles and rolling circle amplification for ultrasensitive live *Salmonella typhimurium* electrochemical biosensing, J. Electroanal. Chem. 826 (2018) 174–180.

[14] F. Li, Z. Yu, X. Han, R.Y. Lai, Electrochemical aptamer-based sensors for food and water analysis: A review, Anal. Chim. Acta 1051 (2019) 1–23.

[15] K. Shanmugasundaram, G. Sai-Anand, A.I. Gopalan, H.G. Lee, H.K. Yeo, S.W. Kang, K.P. Lee, Direct electrochemistry of cytochrome c with three-dimensional nanoarchitectured multicomponent composite electrode and nitrite biosensing, Sensor. Actuat. B Chem. 228 (2016) 737–747.

[16] Z. Wang, P. Tammela, M. Strømme, L. Nyholm, Nanocellulose coupled flexible polypyrrole@graphene oxide composite paper electrodes with high volumetric capacitance, Nanoscale 7 (2015) 3418–3423.

[17] P.A. Palod, V. Singh, Facile synthesis of high density polypyrrole nanofiber network with controllable diameters by one step template free electropolymerization for biosensing applications, Sensor. Actuat. B Chem. 209 (2015) 85–93.

410 [18] Y. Wang, J. Yang, L. Wang, K. Du, Q. Yin, Q. Yin, Polypyrrole/graphene/polyaniline ternary
411 nanocomposite with high thermoelectric power factor, ACS Appl. Mater. Interfaces 9 (2017)
412 20124–20131.
413 [19] R. Sun, H. Chen, Q. Li, Q. Song, X. Zhang, Spontaneous assembly of strong and conductive
414 graphene/polypyrrole hybrid aerogels for energy storage, Nanoscale 6 (2014) 12912–12920.
415 [20] Y. Li, G. Louarn, P.H. Aubert, V. Alain-Rizzo, L. Galmiche, P. Audebert, F. Miomandre,
416 Polypyrrole-modified graphene sheet nanocomposites as new efficient materials for
417 supercapacitors, Carbon 105 (2016) 510–520.
418 [21] J. Zhu, Y. Xu, Enhanced electrochemical performance of polypyrrole depending on
419 morphology and structure optimization by reduced graphene oxide as support frameworks,
420 Electrochim. Acta 265 (2018) 47–55.
421 [22] J. Chen, Y. Wang, J. Cao, Y. Liu, Y. Zhou, J.H. Ouyang, D. Jia, Facile co-electrodeposition
422 method for high-performance supercapacitor based on reduced graphene oxide/polypyrrole
423 composite film, ACS Appl. Mater. Interfaces 9 (2017) 19831–19842.
424 [23] H. Wang, X. Yuan, Y. Wu, X. Chen, L. Leng, H. Wang, H. Li, G. Zeng, Facile synthesis of
425 polypyrrole decorated reduced graphene oxide-Fe_3O_4 magnetic composites and its application
426 for the Cr(VI) removal, Chem. Eng. J. 262 (2015) 597–606.
427 [24] F. Wang, Y. Zhang, Z. Chen, J. Chen, D. Zhang, L. Zhou, Y. Zhao, Polypyrrole/reduced
428 graphene oxide aerogel particle electrodes for high-efficiency electro-catalytic synergistic
429 removal of Cr(VI) and bisphenol A, Chem. Eng. J. 336 (2018) 690–700.
430 [25] P. Pattanayak, N. Pramanik, P. Kumar, P.P. Kundu, Fabrication of cost-effective non-noble
431 metal supported on conducting polymer composite such as copper/polypyrrole graphene oxide

(Cu_2O/PPy–GO) as an anode catalyst for methanol oxidation in DMFC, Int. J. Hydrogen Energy 43 (2018) 11505–11519.

[26] H. Rasouli, L. Naji, M.G. Hosseini, 3D structured polypyrrole/reduced graphene oxide (PPy/rGO)-based electrode ionic soft actuators with improved actuation performance, New J. Chem. 42 (2018) 12104–12118.

[27] D.C. Tiwari, P. Atri, R. Sharma, Sensitive detection of ammonia by reduced graphene oxide/polypyrrole nanocomposites, Synth. Met. 203 (2015) 228–234.

[28] P. Moozarm, W. Pei, F. Lorestani, M.R. Mahmoudian, Y. Alias, Electrodeposition of copper oxide / polypyrrole / reduced graphene oxide as a nonenzymatic glucose biosensor, Sensor. Actuat. B. Chem. 209 (2015) 100–108.

[29] J. Jun, J. Oh, D.H. Shin, S.G. Kim, J.S. Lee, W. Kim, J. Jang, Wireless, Room temperature volatile organic compound sensor based on oolypyrrole nanoparticle immobilized ultrahigh frequency radio frequency identification tag, ACS Appl. Mater. Interfaces 8 (2016) 33139–33147.

[30] M.R. Mahmoudian, Y. Alias, W.J. Basirun, The electrical properties of a sandwich of electrodeposited polypyrrole nanofibers between two layers of reduced graphene oxide nanosheets, Electrochim. Acta 72 (2012) 53–60.

[31] A. Berendjchi, R. Khajavi, A.A. Yousefi, M.E. Yazdanshenas, Surface characteristics of coated polyester fabric with reduced graphene oxide and polypyrrole, Appl. Surf. Sci. 367 (2016) 36–42.

[32] Y. Han, Z. Zhang, M. Yang, T. Li, Y. Wang, A. Cao, Z. Chen, Facile preparation of reduced graphene oxide/polypyrrole nanocomposites with urchin-like microstructure for

wide-potential-window supercapacitors, Electrochim. Acta 289 (2018) 238–247.

[33] X. Yan, X. Zhang, H. Liu, Y. Liu, J. Ding, Y. Liu, Q. Cai, J. Zhang, Fabrication of SDBS intercalated-reduced graphene oxide/polypyrrole nanocomposites for supercapacitors, Synth. Met. 196 (2014) 1–7.

[34] H. Yang, Y. Qiu, X. Guo, Effects of PPy, GO and PPy/GO composites on the negative plate and on the high-rate partial-state-of-charge performance of lead-acid batteries, Electrochim. Acta 215 (2016) 346–356.

[35] G. Gnana Kumar, C.J. Kirubaharan, S. Udhayakumar, K. Ramachandran, C. Karthikeyan, R. Renganathan, K.S. Nahm, Synthesis, structural, and morphological characterizations of reduced graphene oxide-supported polypyrrole anode catalysts for improved microbial fuel cell performances, ACS Sustain. Chem. Eng. 2 (2014) 2283–2290.

[36] X. Cao, Y. Ye, S. Liu, Gold nanoparticle-based signal amplification for biosensing, Anal. Biochem. 417 (2011) 1–16.

[37] Y. Ye, J. Gao, H. Zhuang, H. Zheng, H. Sun, Y. Ye, X. Xu, X. Cao, Electrochemical gene sensor based on a glassy carbon electrode modified with hemin-functionalized reduced graphene oxide and gold nanoparticle-immobilized probe DNA, Microchim. Acta. 184 (2017) 245–252.

[38] Y. Ye, J. Xie, Y. Ye, X. Cao, H. Zheng, X. Xu, Q. Zhang, A label-free electrochemical DNA biosensor based on thionine functionalized reduced graphene oxide, Carbon 129 (2018) 730–737.

[39] C. Yu, Y. Yu, J. He, L. Zhang, Y. Zhao, J. Wu, Y. Niu, J. Chen, A novel non-invasive detection method for the FGFR3 gene mutation in maternal plasma for a fetal achondroplasia

diagnosis based on signal amplification by hemin-MOFs/PtNPs, Biosens. Bioelectron. 91 (2017) 892–899.

[40] Y. Chen, J. Li, L. Tan, Q. Li, X. Zhang, H. Xu, Electrodeposition of polypyrrole/functionalized-multiwalled carbon nanotubes composite and its application in supercapacitors, Electrochim. Acta 258 (2017) 43–50.

[41] F. Kiani, N.A. Astani, R. Rahighi, A. Tayyebi, M. Tayebi, J. Khezri, E. Hashemi, U. Rothlisberger, A. Simchi, Effect of graphene oxide nanosheets on visible light-assisted antibacterial activity of vertically-aligned copper oxide nanowire arrays, J. Colloid Interface Sci. 521 (2018) 119–131.

[42] Y. Ye, S. Ding, Y. Ye, H. Xu, X. Cao, S. Liu, H. Sun, Enzyme-based sensing of glucose using a glassy carbon electrode modified with a one-pot synthesized nanocomposite consisting of chitosan, reduced graphene oxide and gold nanoparticles, Microchim. Acta (2015) 1783–1789.

[43] G.G. Kumar, C.J. Kirubaharan, S. Udhayakumar, K. Ramachandran, C. Karthikeyan, R. Renganathan, K.S. Nahm, Synthesis, structural, and morphological characterizations of reduced graphene oxide-supported polypyrrole anode catalysts for improved microbial fuel cell performances, ACS Sustain. Chem. Eng. 2 (2014) 2283–2290.

[44] K. Deshmukh, M.B. Ahamed, S.K.K. Pasha, R.R. Deshmukh, P.R. Bhagat, Highly dispersible graphene oxide reinforced polypyrrole/polyvinyl alcohol blend nanocomposites with high dielectric constant and low dielectric loss, RSC Adv. 5 (2015) 61933–61945.

[45] S. Konwer, R. Boruah, S.K. Dolui, Studies on conducting polypyrrole/graphene oxide composites as supercapacitor electrode, J. Electron. Mater. 40 (2011) 2248–2255.

[46] G. Kim, J.H. Moon, C.Y. Moh, J. guk Lim, A microfluidic nano-biosensor for the detection of

pathogenic Salmonella, Biosens. Bioelectron. 67 (2015) 243–247.

[47] S. Srinivasan, V. Ranganathan, M.C. DeRosa, B.M. Murari, Label-free aptasensors based on fluorescent screening assays for the detection of *Salmonella typhimurium*, Anal. Biochem. 559 (2018) 17–23.

[48] D. Kyprianou, A.R. Guerreiro, M. Nirschl, I. Chianella, S. Subrahmanyam, A.P.F. Turner, S. Piletsky, The application of polythiol molecules for protein immobilisation on sensor surfaces, Biosens. Bioelectron. 25 (2010) 1049–1055.

[49] R. Mutreja, M. Jariyal, P. Pathania, A. Sharma, D.K. Sahoo, C.R. Suri, Novel surface antigen based impedimetric immunosensor for detection of *Salmonella typhimurium* in water and juice samples, Biosens. Bioelectron. 85 (2016) 707–713.

[50] E. Sheikhzadeh, M. Chamsaz, A.P.F. Turner, E.W.H. Jager, V. Beni, Label-free impedimetric biosensor for *Salmonella typhimurium* detection based on poly [pyrrole-co-3-carboxyl-pyrrole] copolymer supported aptamer, Biosens. Bioelectron. 80 (2016) 194–200.

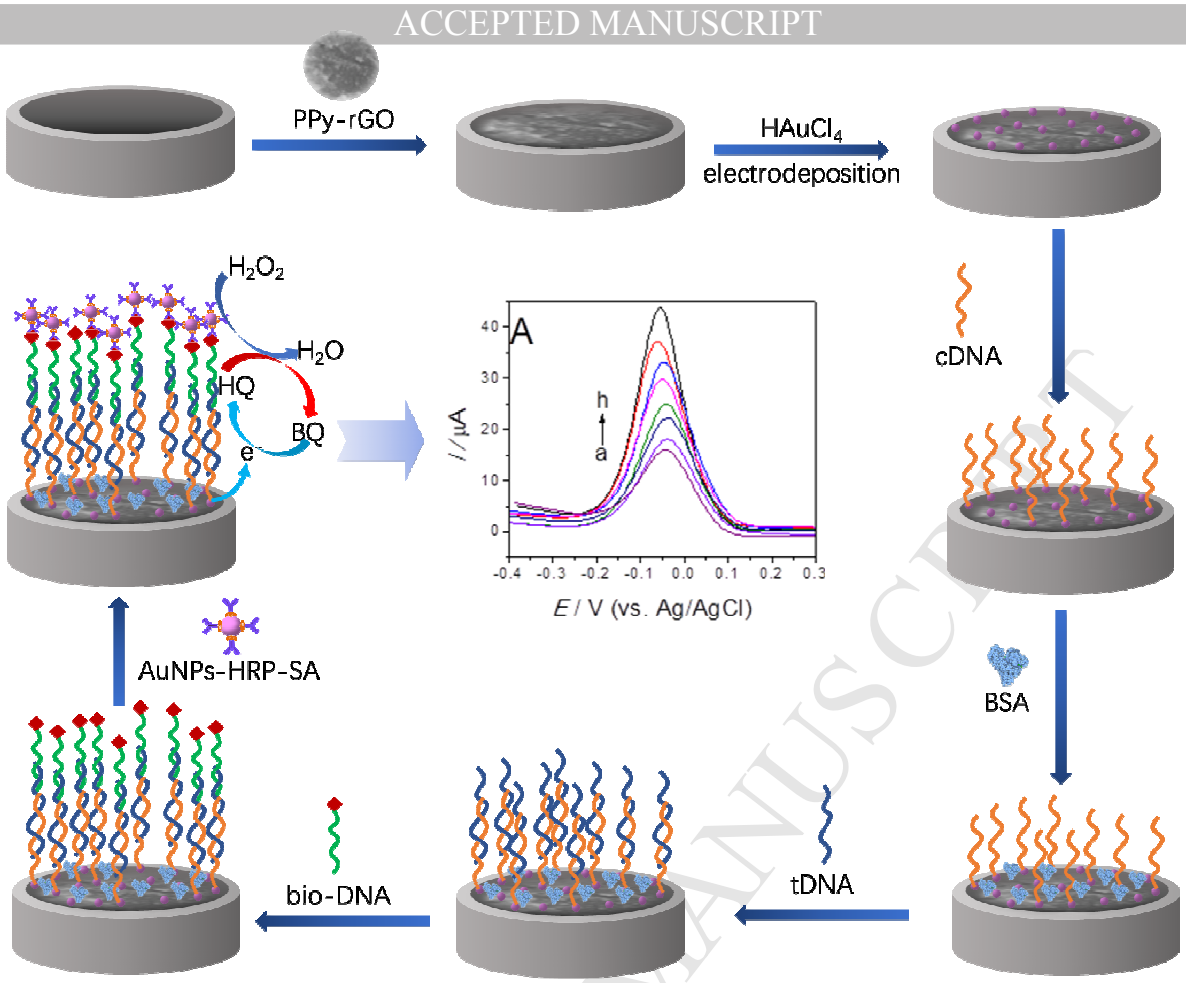

Scheme 1 The designed strategy for the detection of *Salmonella invA* gene.

Fig. 1. SEM images of GO (A), rGO (B), and PPy-rGO (C).

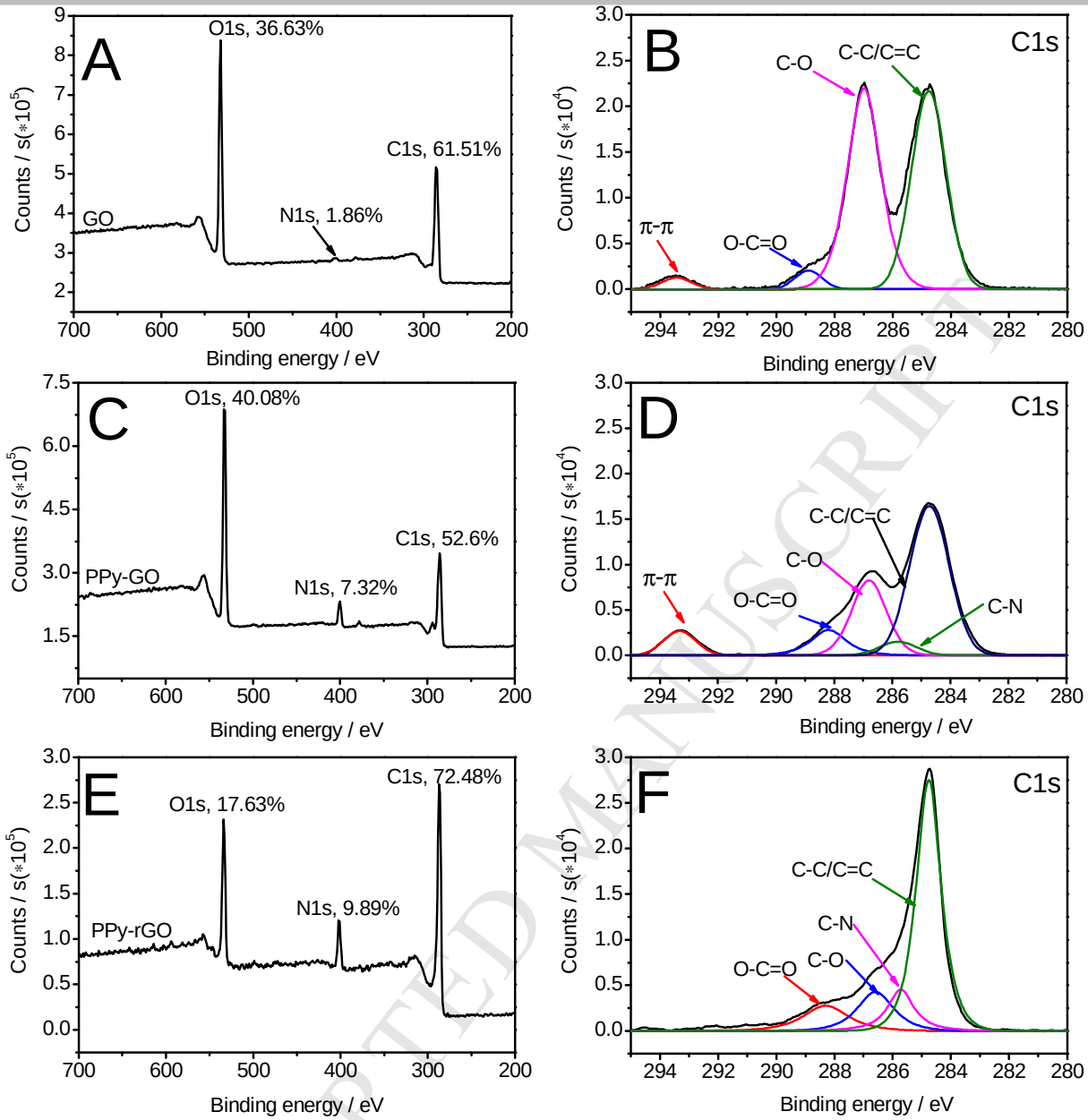

Fig. 2. XPS spectra of GO, PPy-GO and PPy-rGO. (A) Full survey spectrum of GO. (B) C1s spectrum in GO. (C) Full survey spectrum of PPy-GO. (D) C1s spectrum in PPy-GO. (E) Full survey spectrum of PPy-rGO. (F) C1s spectrum in PPy-rGO.

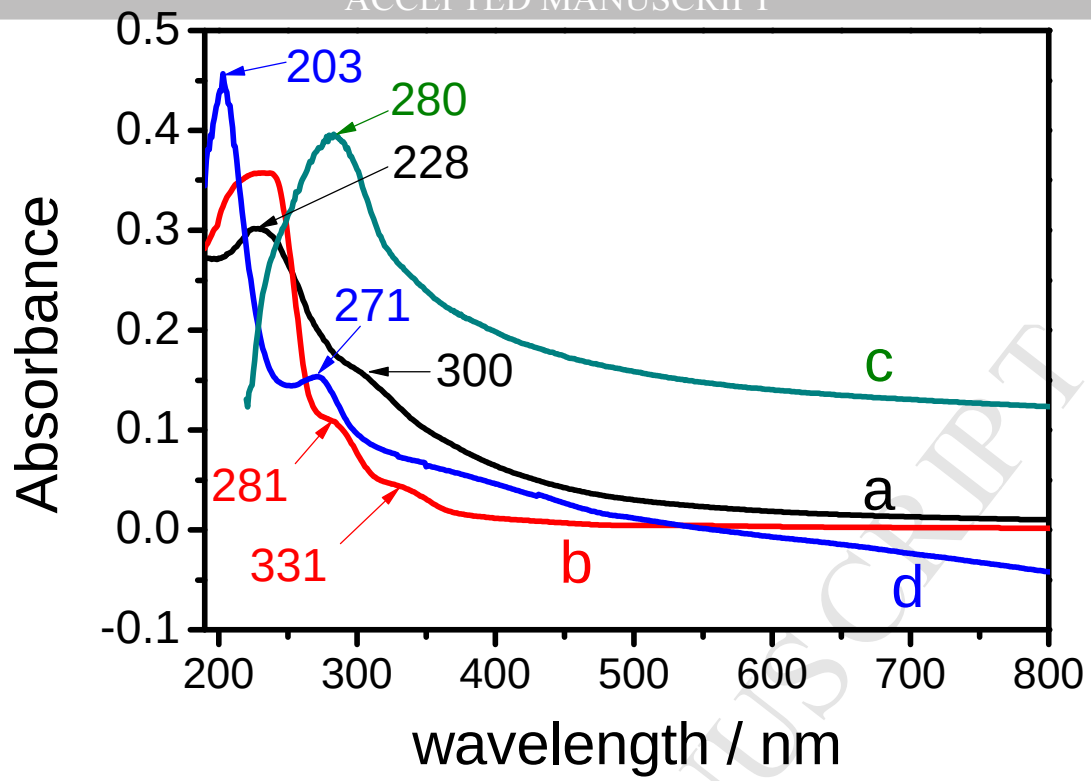

Fig. 3. UV-vis spectra of GO (a), PPy-GO (b), rGO (c), and PPy-rGO (d).

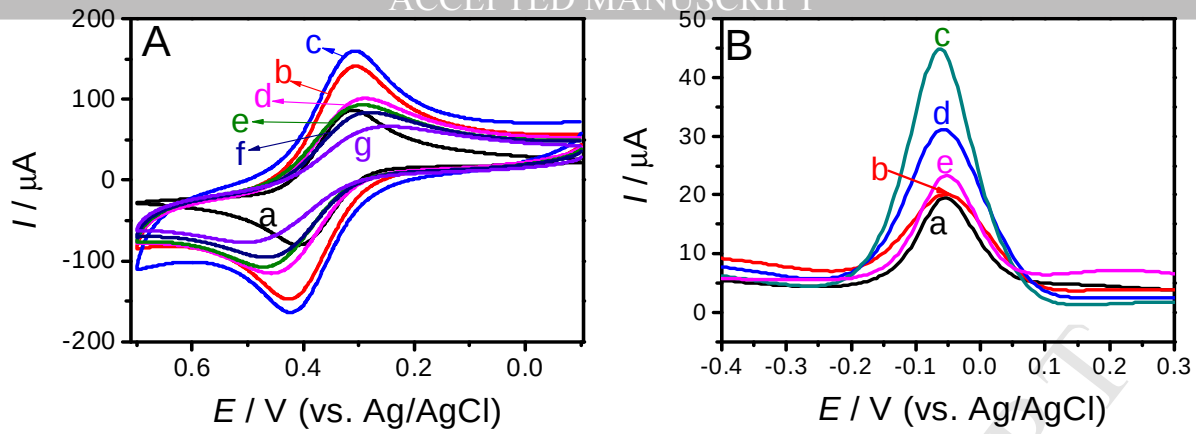

Fig. 4. (A) CVs recorded at bare GCE (a), PPy-rGO/GCE (b), depAuNPs/PPy-rGO/GCE (c), cDNA/depAuNPs/PPy-rGO/GCE (d), cDNA/depAuNPs/PPy-rGO/GCE blocked with BSA (e), bio-DNA/tDNA/cDNA/depAuNPs/PPy-rGO/GCE (f), and AuNPs-HRP-SA/bio-DNA/tDNA/cDNA/depAuNPs/PPy-rGO/GCE (g) in 5.0 mM $[Fe(CN)_6]^{3-/4-}$ containing 0.1 M KCl. (B) DPV responses obtained on different electrodes in 0.1 M PBS (pH 7.4) containing 2.0 mM of HQ and 3.0 mM of H_2O_2. (a) blank control of the constructed sensing electrode. (b) the constructed sensing electrode in detection of tDNA without help from AuNPs-HRP-SA. (c) the constructed sensing electrode in detection of tDNA. (d) the constructed sensing electrode in detection of tDNA without signal amplification of AuNPs. (e) the electrode of cDNA/depAuNPs/rGO/GCE in detection of tDNA without signal amplification of AuNPs. The concentration of tDNA was 100 pM.

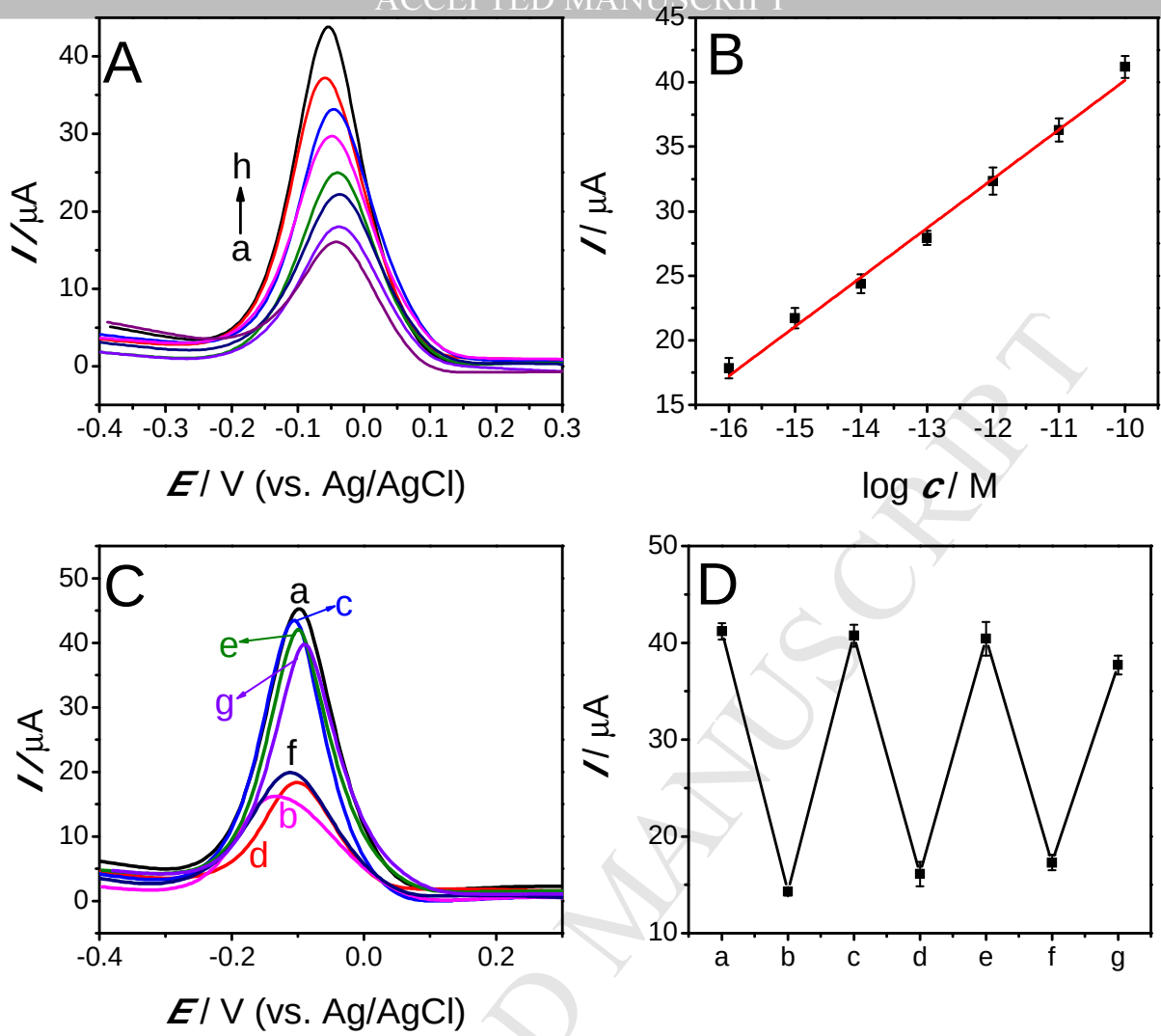

Fig. 5. (A) Typical DPV curves for different concentrations of the tDNA: (a) 0 M, (b) 1.0×10^{-16} M, (c) 1.0×10^{-15} M, (d) 1.0×10^{-14} M, (e) 1.0×10^{-13} M, (f) 1.0×10^{-12} M, (g) 1.0×10^{-11} M, and (f) 1.0×10^{-10} M. (B) Linear relationship between the current responses and the logarithm of tDNA concentration. (C) Regeneration ability of the biosensor toward tDNA of 100 pM. (a), (c), (e) and (g) were the DPV responses of the initial, 1st regeneration, 2nd regeneration and 3rd regeneration, respectively. (b), (d) and (f) were the blank signal of 1st regeneration, 2nd regeneration and 3rd regeneration, respectively.

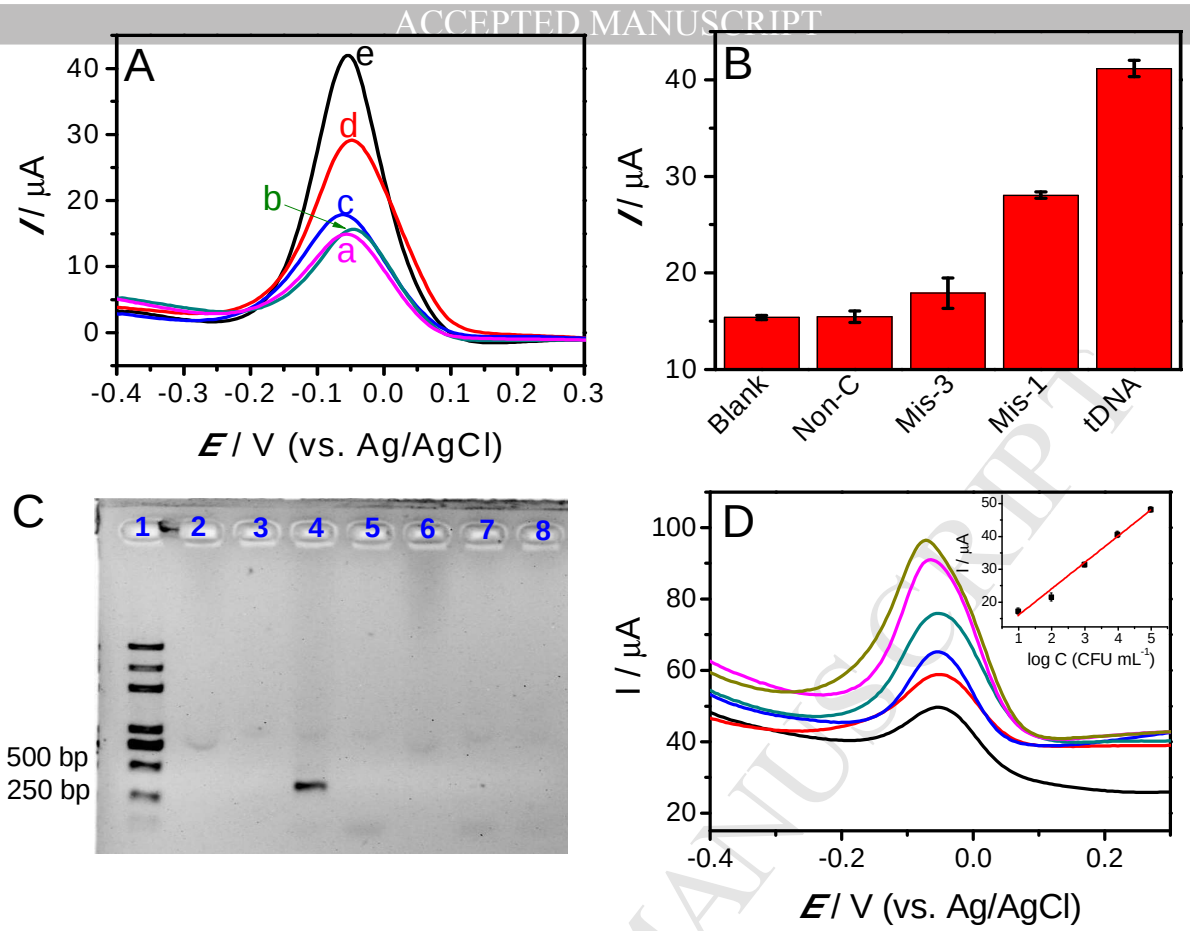

Fig. 6. (A) Selectivity of the biosensor toward different DNA sequences. (a) Blank, (b) the non-complementary sequence, (c) the Mis-3, (d) the Mis-1, and (e) tDNA. (B) Histogram of the corresponding peak current values in (A). (C) Agarose gel electrophoresis for marker (lane 1), PCR products without primers (lane 2) and exacted total DNA (lane 3), and PCR products of 9.6×10^{4} CFU mL^{-1} (lane 4), 9.6×10^{3} CFU mL^{-1} (lane 5), 9.6×10^{2} CFU mL^{-1} (lane 6), 9.6×10^{1} CFU mL^{-1} (lane 7), 9.6 CFU mL^{-1} (lane 8). (D) DPV responses of the biosensor in detection of *Salmonella*. From top to bottom: 9.6×10^{4} CFU mL^{-1}, 9.6×10^{3} CFU mL^{-1}, 9.6×10^{2} CFU mL^{-1}, 9.6×10^{1} CFU mL^{-1}, 9.6 CFU mL^{-1}, and 0 CFU mL^{-1}. Inset: the resulting calibration curves of *I vs*. log *C* (CFU mL^{-1}).

Table 1. Comparison in analytical performance between present method and other reported biosensors for *Salmonella* detection.

Methods	LOD (CFU mL^{-1})	Linear range (CFU mL^{-1})	Detection time* (h)	Refs
Colorimetric immunoassay	3×10^3	$3\times10^3 – 3\times10^6$	5	[1]
Fluorescence biosensor	10^3	$0 – 10^6$	2	[46]
Label-free fluorescent aptasensor	464	1530 – 96938	--	[47]
Surface plasmon resonance (SPR) sensor	5×10^6	--	10	[48]
Electrochemical (impedimetric) immunosensor	10	$10 – 10^5$	2	[49]
Electrochemical (DPV) genosensor using rolling circle amplification and signal nanoprobe	6	$6 – 6\times10^8$	--	[8]
Electrochemical (impedimetric) aptasensor	3	$10^2 – 10^8$	1.5	[50]
Electrochemical (DPV) genosensor	**8.07**	**$9.6 – 9.6\times10^4$**	**2**	**This work**

* The detection time includes the time for hybridization and electrochemical measurements.

Highlights:

- Polyrrole-reduced graphene oxide nanocomposite was prepared and used to facilitate electron transfer in constructing the *Salmonella* biosensor.
- AuNPs-horseradish peroxidase-streptavidin was used as nanotag for signal amplification.
- The fabricated biosensor can detect *invA* gene sequence with LOD of 4.7×10^{-17} M.
- The biosensor was used to detect *Salmonella* with LOD of 8.07 CFU mL^{-1}.

Conflict of interest statement

We declare that we have no financial and personal relationships with other people or organizations that can inappropriately influence our work, there is no professional or other personal interest of any nature or kind in any product, service and/or company that could be construed as influencing the position presented in, or the review of, the manuscript entitled, “Electrochemical detection for Salmonella using an invA genosensor on polypyrrole-reduced graphene oxide modified glassy carbon electrode and AuNPs-horseradish peroxidase-streptavidin as nanotag”.

Xiaodong Cao

Ph.D.

Associate Professor of Food Science and Engineering,

Hefei University of Technology

Hefei, 230009

China